JOURNAL OF MATERIALS SCIENCE 18 (1983) 3281–3287

The effect of interfacial adhesion on the mechanism for craze formation in polystyrene–glass bead composites

M. E. J. DEKKERS, D. HEIKENS
Eindhoven University of Technology, Laboratory of Polymer Technology, P.O.B. 513, 5600 MB Eindhoven, The Netherlands

The craze formation in polystyrene–glass bead composites subjected to a uniaxial tension has been investigated. To gain insight into the role of interfacial adhesion, the bonding between glass and polystyrene was varied by using different silane coupling agents. The distributions of several craze formation criteria around an isolated adhering glass sphere in a polystyrene matrix have been computed with the aid of the finite element analysis. It was found that the mechanism for craze formation is fundamentally different for adhering and non-adhering glass beads. In the case of excellent interfacial adhesion the crazes form near the poles of the beads in regions of maximum dilatation and of maximum principal stress. With poor interfacial adhesion the crazes form at the interface between pole and equator. It is proposed that in the latter case craze formation is preceeded by dewetting along the phase boundary.

1. Introduction

When a craze-prone plastic is subjected to mechanical deformation, the crazes form at stress concentrating heterogeneities in the material. Many details concerning crazing are given in a number of comprehensive reviews [1, 2]. An interesting feature is the criterion for craze formation. It has been suggested that crazes form in the material when a critical limit is reached in for instance stress [3], stress bias [4], strain [5], distortion strain energy [6], dilatation [7] or strain energy [8]. A method for comparing the various proposed criteria was executed by Wang *et al.* [8]. In this work a polystyrene (PS) sample containing an embedded steel ball (diameter = 3×10^{-3} m) was subjected to a uniaxial tension. The crazes were observed to originate at the surface of the ball in regions of maximum strain and of maximum strain energy. After this, the crazes expanded into the matrix in the direction perpendicular to the applied tension.

In this article the results of an investigation into the craze formation at another rigid inclusion, namely glass beads (average diameter = 3×10^{-5} m) dispersed in a PS matrix are presented. Because the crazing behaviour of composites with PS as the matrix material is known to be strongly influenced by the degree of interfacial adhesion [9], two situations are considered in the present study: poor and excellent interfacial adhesion. The bonding between glass and PS is varied by treating the surface of the glass chemically using two different silane coupling agents.

In order to analyse the distributions of a number of craze formation criteria around an adhering glass sphere in PS, the three-dimensional stress distribution (due to uniaxial tension) is computed by applying the finite element method. The results obtained in this study will be compared with the results reported by Wang *et al.* [8].

2. Experimental details

The composites consisting of PS and glass beads were prepared by meltmixing on a laboratory mill at 190°C. The PS used was Styron 634 with a number average molar mass, $\bar{M}_n$, of about 1×10^5

0022–2461/83 $03.00 + .12

(Dow Chemical Co.). The glass beads (Tamson 31/20) have a diameter range of 1.0×10^{-5} to 5.3×10^{-5} m and a specific gravity of 2.48.

Before being dispersed in PS, the glass beads were surface treated with two different silane coupling agents: a cationic vinylbenzyl trimethoxysilane $[(CH_3O)_3Si(CH_2)_3NH(CH_2)_2NHCH_2{-}C_6H_4{-}CH_1{=}CH_2 \cdot HCl]$ (Dow Corning Z-6032) obtained from Mavom, The Netherlands, and vinyltriethoxysilane (Fluka). As pointed out by Plueddeman [10] the first should yield excellent interfacial adhesion between glass and PS in contrast with vinylsilane.

The silanes were applied as follows: first the glass beads were cleaned by refluxing isopropyl alcohol for 2 h and vacuum dried for 1 h at 130° C.

1. *Cationic vinylbenzylsilane:* 75 g of refluxed glass was stirred for 1 h at room temperature in a 5% solution of silane in methanol containing 1% concentrated hydrochloric acid and 1% dicumylperoxide (totally 200 ml).

2. *Vinylsilane:* 75 g of refluxed glass was stirred for 1 h at room temperature in a 2% solution of silane in a 50/50 mixture of ethanol and water containing 1% concentrated hydrochloric acid (totally 200 ml).

After this, the glass was allowed to air dry for 1 h and cured for 1 h at 100° C under vacuum. Then the glass beads were ready to be melt-mixed with PS.

Tensile specimens were machined in accordance with ASTM D 638 III from compression moulded sheets. To reduce thermal stresses the specimens were annealed at 80° C for 24 h. Then conditioned at 20° C and 65% relative humidity for at least 48 h before testing. The tensile tests were performed until fracture on an Instron tensile tester at a crosshead speed of 2×10^{-3} m min^{-1}. The gauge length was 10^{-1} m.

In order to investigate the degree of interfacial adhesion between glass and PS, fracture surfaces of specimens containing 10 vol% of glass were examined with a Cambridge scanning electron microscope. Specimens strained uniaxially in a tensile test and containing 0.5 vol% of glass were examined with a Zeiss light microscope. As these specimens are transparent the crazes, formed at the glass beads during the tensile test, are well visible.

3. Results

The difference in PS–glass adhesion due to the treatment with various silanes is shown by the fracture surfaces in Fig. 1. The beads treated with vinylsilane are essentially free of any adhering PS. This means that vinylsilane hardly yields any interfacial adhesion. This in contrast with a coating of cationic vinylbenzylsilane where a lot of matrix material has remained on the beads indicating excellent interfacial adhesion.

The degree of interfacial adhesion has consequences for the location near the surface of the glass bead at which the craze originates during the tensile test. In Fig. 2 details of light microscope photographs of crazed samples are shown. Fig. 2a

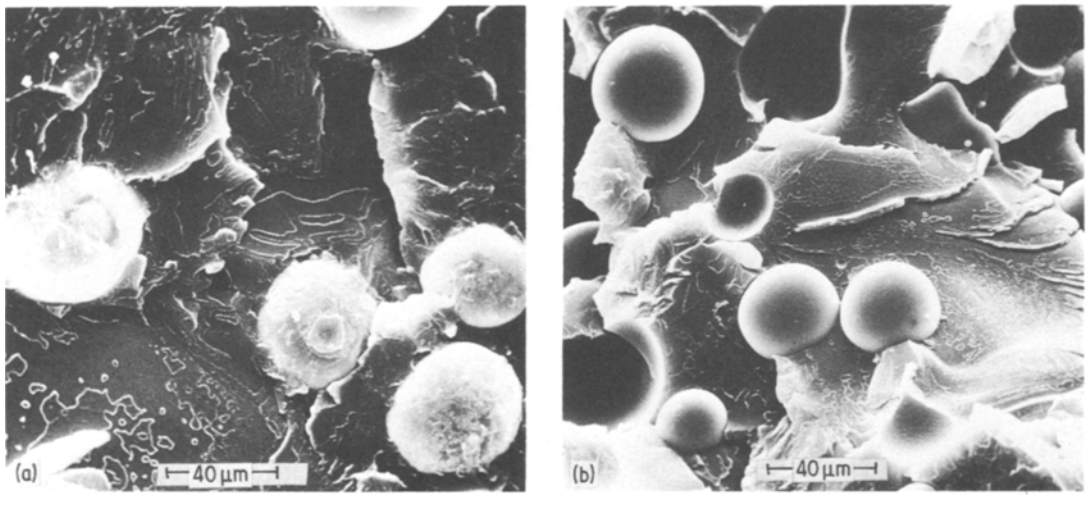

Figure 1 Scanning electron micrographs of fracture surfaces of PS–glass bead composites (90/10 by volume). (a) Cationic vinylbenzylsilane treated beads show excellent interfacial adhesion. (b) Vinylsilane treated beads show poor interfacial adhesion.

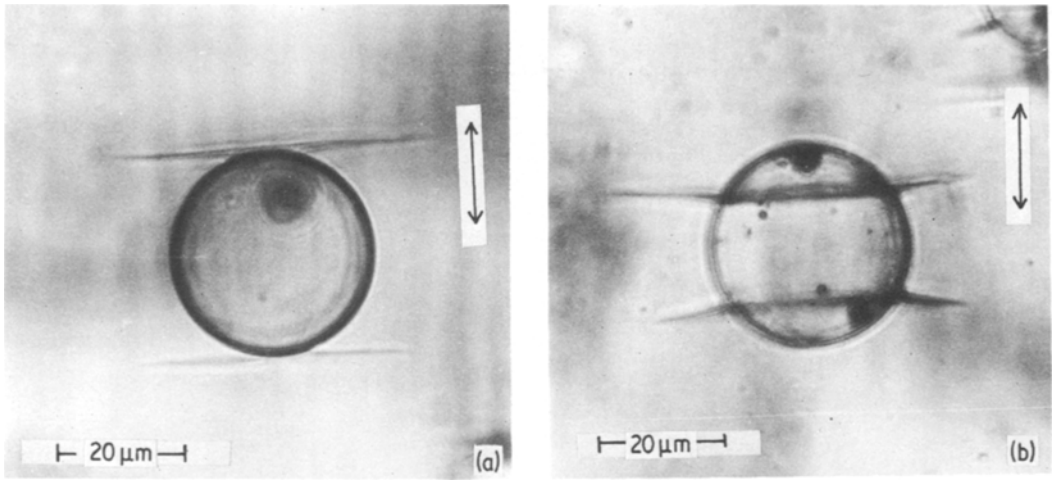

Figure 2 Light micrographs of craze patterns around (a) an excellent adhering glass bead and (b) a poor adhering glass bead. The arrow indicates the direction of the applied tension.

shows that in the case of excellent interfacial adhesion the craze forms near the pole of the bead. With poor interfacial adhesion the craze forms at about 60° from the pole defined by symmetry of axis of the stressed sphere.

4. Analysis

4.1. Finite element method

In order to calculate the distributions of a number of craze formation criteria, the three-dimensional stress situation (due to uniaxial tension) around an adhering isolated glass sphere in a PS matrix must be known. In the present investigation this stress situation was numerically computed using the finite element analysis for axisymmetric solids. An available computer program written by Peters [11] made it possible to apply this method. The principles of the finite element analysis are treated in detail elsewhere [12]. The application of the axisymmetric analysis for spherically filled materials has been described by Broutman and Panizza [13]. As the procedure followed in this study is similar to that followed by Broutman and Panizza, the interested reader is referred to this work for details.

The applied method is based on the assumption that both filler and matrix obey elastic stress–strain relations and that perfect bonding exists between filler and matrix. It is important to realize that this last assumption implies that the results of the analysis may only be compared with the situation of excellent interfacial adhesion between PS and glass.

The analysis did not take into account a possible interfacial interlayer caused by the silane treatment. In practice such an interlayer is assumed to be thin enough to be neglected.

In the analysed system the glass occupies three volume per cent. As it was already pointed out, at that low percentage no interaction exists between the spheres [13], and therefore the investigated system represents the situation of isolated glass spheres dispersed in a PS matrix.

The elastic constants used are:

PS : Young's modulus 3250 MPa
Poisson's ratio 0.34
glass: Young's modulus 70000 MPa
Poisson's ratio 0.22.

The applied tension was taken at 20 MPa because at about this stress level the crazes start to form in PS–glass bead composites with excellent interfacial adhesion [14].

It should be noted that stresses in the composite are not only set up by applied tension but also by differential thermal contraction, because the coefficient of thermal expansion of glass is smaller than that of PS (α glass $= 7 \times 10^{-6} K^{-1}$, α PS $= 7 \times 10^{-5} K^{-1}$). For this reason the stresses around the glass bead induced by cooling from the annealing temperature to room temperature (temperature difference 60° C) were also calculated using the equations derived by Beck *et al.* [15]. The maximum value of the radial thermal compressive stress was found to be 5.6 MPa. The thermal stresses have been superimposed on the stresses due to uniaxial tension computed by

finite element analysis. This resulted in the stress distribution around an isolated adhering glass sphere in a PS matrix which takes both thermal and mechanical factors into account.

4.2. Craze formation criteria

The distributions of the following craze formation criteria along the interface and near the poles of an adhering glass sphere in a PS matrix have been calculated:

1. maximum principal stress σ;
2. maximum principal strain ϵ;
3. maximum principal shear stress τ;
4. maximum dilatation Δ;
5. maximum strain energy per unit volume W_S;
6. maximum distortion strain energy per unit volume W_D.

The expressions of these criteria in terms of the principal stresses in the three-dimensional complex stress system can be found elsewhere [8, 16].

The stress-bias criterion [4] has not been considered because this criterium involves two material constants which cannot be determined by the simple uniaxial tensile test executed in this study.

Fig. 3 shows the geometric arrangement for the spherical inclusion with radius R_0 in a matrix under uniaxial tension. The pole of the sphere is defined by $R/R_0 = 1$ and $\theta = 0$ (or $\theta = 180°$). In Fig. 4 the distributions of the various criteria along the interface at $R/R_0 = 1$ are plotted. In Table I for each criterion both the angle θ at which the maximum was found and the relative value of that maximum are listed. Fig. 5 shows the distributions of the various criteria along the polar axis ($\theta = 0$). The relative distances R/R_0 from the pole at which the maxima were found and the relative values of those maxima are also given in Table I. It should be noted that calculations for the PS–glass bead system without thermal stresses did not change the positions of the maxima or the shape of the curves significantly.

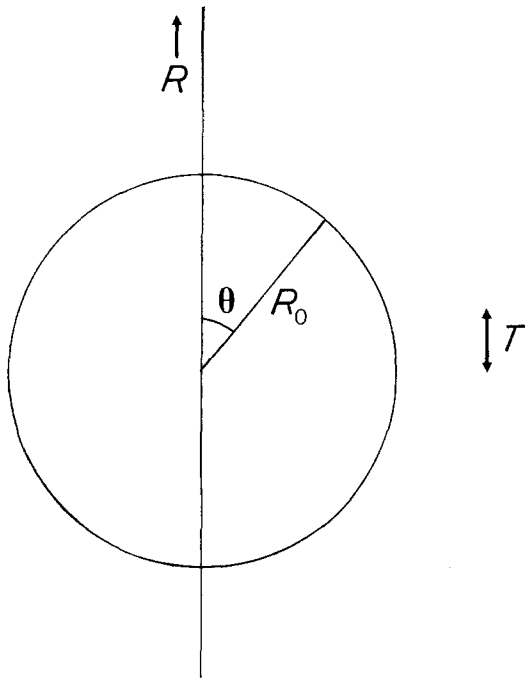

Figure 3 The geometric arrangement for a spherical inclusion with radius R_0. The arrow indicates the direction of the applied tension T.

5. Discussion

5.1. Craze formation at the excellent adhering glass bead

In the case of excellent interfacial adhesion, the crazes form near the poles of the glass bead as shown by Fig. 2a. Because of the excellent interfacial adhesion it is allowed to compare this craze pattern with the calculated distributions of craze formation criteria based on perfect interfacial bonding.

From Fig. 4 and Table I it appears that, directly at the phase boundary at $R/R_0 = 1$, only the criteria principal stress and dilatation (sum of principal strains) have maximum values at $\theta = 0°$. The other investigated criteria have maxima along the interface at angles relatively far remote from the poles.

From Fig. 2a it cannot be determined if the craze originates directly at the phase boundary or somewhat outwards in the matrix. Therefore the distributions of criteria along the polar axis at $\theta = 0$ have also been investigated. Fig. 5 and Table I show the results: Dilatation has its maximum directly at the phase boundary at $R/R_0 = 1$. The maximum of the principal stress lies at short distance from the phase boundary at $R/R_0 = 1.1$ to 1.2. This is rather close to the sphere so that, based on the craze pattern of Fig. 2a, principal stress cannot be ruled out completely as possible craze formation criterion. As the other four investigated criteria have maxima along the polar axis at distances relatively far away from the sphere ($R/R_0 > 1.3$), these criteria should definitely be excluded as craze formation criterion in the present case.

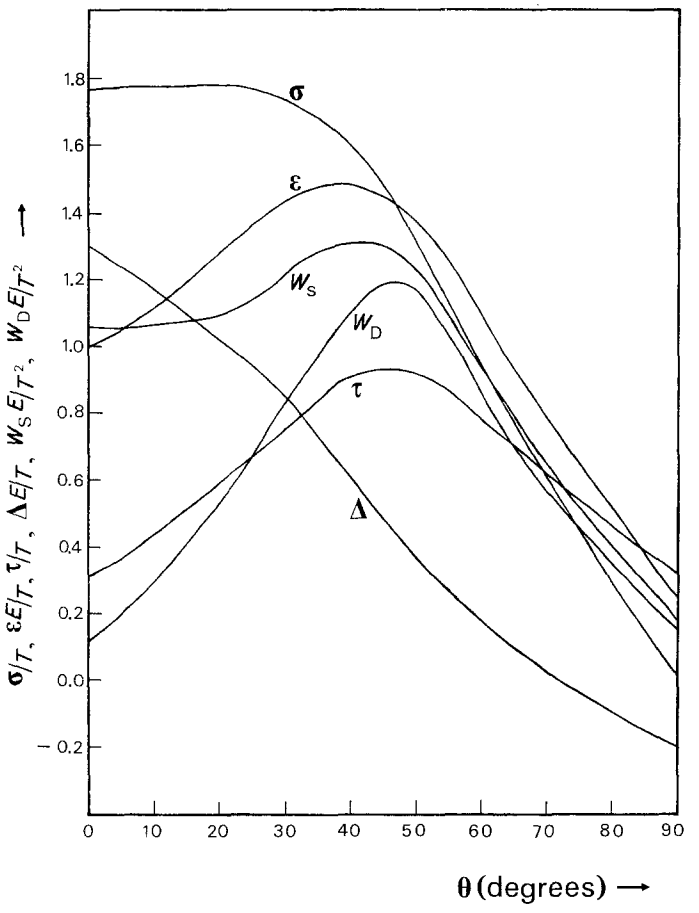

Figure 4 Distributions of major principal stress (σ), major principal strain (ϵ), major principal shear stress (τ), dilatation (Δ), strain energy density (W_S) and distortion strain energy density (W_D) along the PS–glass interface at $R/R_0 = 1$. E and T are, respectively, the Young's modulus of PS and the applied tension (20 MPa). The maximum thermal stress was assumed to be 5.6 MPa.

5.2. Craze formation at the steel ball

As pointed out before Wang *et al.* [8] have investigated the distributions of craze formation criteria along the interface of another rigid spherical inclusion, namely, a steel ball embedded in PS. To calculate the stress distribution around a steel sphere, they used Goodier's equations [17] which are, like the finite element analysis, also based on perfect interfacial adhesion. The distributions of criteria obtained in this way are very similar to those shown in Fig. 4. This proves the applicability of the axisymmetric finite element analysis for computing three-dimensional stress distributions around spherical inclusions.

However, in the case of the steel ball the crazes did not form near the poles, as is the case with adhering glass beads, but at an angle θ of about 37°. Based on this result Wang concluded that crazes form in regions of maximum principal strain and of maximum strain energy. But, the results of the present study prompt the present authors to believe that this conclusion is based on false arguments. The craze pattern around the steel ball resembles the craze pattern around the

TABLE I Maxima of craze formation criteria along the interface at $R/R_0 = 1$ and along the polar axis at $\theta = 0$. The values of the applied tension and the maximum thermal stress are, respectively, 20 and 5.6 MPa

Criterion	θ_{max} ($R/R_0 = 1$)	Relative value at θ_{max}	$R/R_{0\,max}$ ($\theta = 0$)	Relative value at $R/R_{0\,max}$
Principal stress σ	0–25	1.77	1.1–1.2	1.87
Principal strain ϵ	38	1.48	1.33	1.59
Principal shear stress τ	46	0.94	1.37	0.73
Dilatation Δ	0	1.29	1.0	1.29
Strain energy density W_S	41	1.32	1.31	1.31
Distortion strain energy density W_D	45	1.20	1.37	0.97

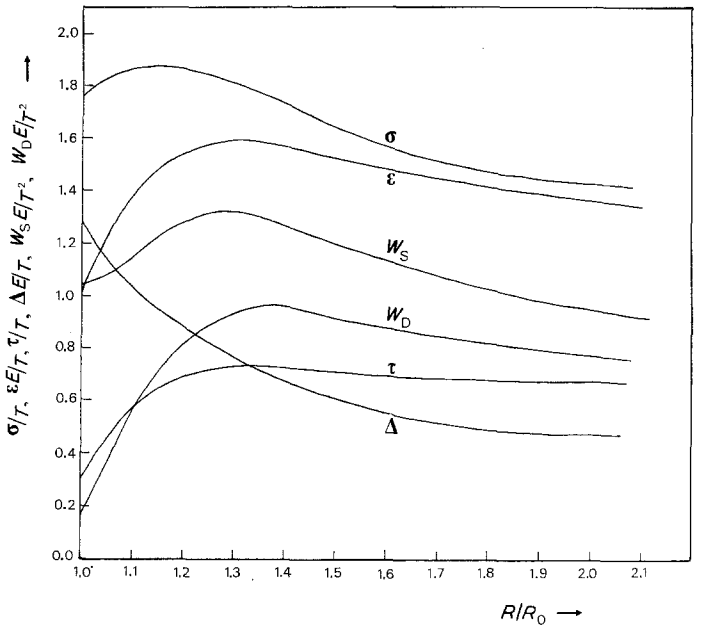

Figure 5 Distributions of major principal stress (σ), major principal strain (ϵ), major principal shear stress (τ), dilatation (Δ), strain energy density (W_S) and distortion strain energy density (W_D) along the polar axis at $\theta = 0$. E and T are, respectively, the Young's modulus of PS and the applied tension (20 MPa). The maximum thermal stress was assumed to be 5.6 MPa.

poor adhering glass bead shown in Fig. 2b namely much more, than that around the excellent adhering glass bead shown in Fig. 2a. Therefore it is doubted that the adhesion between steel and PS was good enough to allow comparison of the experimental results with the calculated distributions of craze criteria around the steel sphere based on perfect interfacial bonding.

The mechanism for craze formation at poor adhering rigid spherical inclusions in a PS matrix will be discussed in the next section.

5.3. Craze formation at the poor adhering glass bead

Fig. 2b shows the craze pattern around the glass bead with poor interfacial adhesion. The crazes originate at an angle θ of about 60°. This indicates another mechanism for craze formation compared with the excellent adhering glass bead.

Due to differential thermal contraction a negative radial stress field exists around the sphere. By applying a uniaxial external tension this negative radial stress is first balanced at the poles. It is now suggested that at this particular moment, in the case of the poor adhering sphere, separation between glass and matrix occurs at the poles (dewetting). By continuing the tensile test the dewetting proceeds along the phase boundary in the direction of the equator, and because of that a small cap-shaped cavity is formed which lies around the top of the sphere. As the sharp edge of this cavity gradually approaches the equator, dewetting becomes more difficult in consequence of the contraction of the matrix perpendicular to the applied tension. At a certain angle θ dewetting stops because it is energetically more favourable to start a craze at the edge of the cavity. The angle at which the craze forms is supposed to depend on several factors: the degree of interfacial adhesion, the (elastic) properties of matrix and rigid filler and under certain circumstances the diameter of the inclusion [18]. The exact role of these factors has to be investigated further.

Resuming, the essence of the discussion above is that in the case of poor adhesion the formation of crazes is preceeded by dewetting along the interface between sphere and matrix.

6. Conclusion

In the case of excellent interfacial adhesion the crazes form near the poles of the glass beads in regions of maximum dilatation and of maximum principal stress. Based on the results of the applied method, a definite choice between both craze formation criteria cannot be made. It should be remembered that in this study only a few simple criteria are considered. Other more complicated criteria could not be investigated by the applied method, e.g. the empirical stress-bias criterion which actually is an extension of the dilatation criterion. Therefore a combination of the dilatation criterion with the principal stress criterion or some of the other criteria should not be ruled out. Anyhow, from the present investigations it

can be concluded that dilatation plays an important role in craze formation. This is logical as craze formation is inhibited by hydrostatic compression and only can occur under tension through the production of voids.

With poor interfacial adhesion the crazes form at the interface between pole and equator. It is proposed that in this case craze formation is preceeded by dewetting along the phase boundary.

Thus it appears that the mechanism for craze formation is fundamentally different for adhering and non-adhering glass beads in a PS matrix. The consequences of this on the mechanical behaviour of PS–glass composites will be reported in a subsequent paper [14].

Acknowledgements

The authors would like to thank L. H. Braak for his advice concerning the finite element analysis. The assistance of H. C. B. Ladan in obtaining the optical micrographs is also gratefully acknowledged.

References

1. R. P. KAMBOUR, *J. Polym. Sci. Macromol. Rev.* 7 (1973) 1.
2. C. B. BUCKNALL, "Toughened Plastics" (Applied Science Publishers Ltd., London, 1977).
3. C. B. BUCKNALL and R. R. SMITH, *Polymer* **6** (1965) 437.
4. S. S. STERNSTEIN and L. ONGCHIN, *ACS Prepr.* **10** (1969) 1117.
5. B. MAXWELL and L. F. RAHM, *Ind. Eng. Chem.* **41** (1948) 1988.
6. S. MATSUOKA, J. H. DAANE, T. K. KWEI and T. W. HUSEBY, *ACS Prepr.* **10** (1969) 1198.
7. S. STRELLA, *J. Polym. Sci. A-2* **4** (1966) 527.
8. T. T. WANG, M. MATSUO and T. K. KWEI, *J. Appl. Phys.* **42** (1971) 4188.
9. S. D. SJOERDSMA, M. E. J. DEKKERS and D. HEIKENS, *J. Mater. Sci.* **17** (1982) 2605.
10. E. P. PLUEDDEMAN, *Appl. Pol. Symp.* **19** (1972) 75.
11. F. J. PETERS, Femsys, a system for calculations based on the finite element method part I, TH Eindhoven, Department of Mathematics, 1976 (in Dutch).
12. O. C. ZIENKIEWISZ, "The Finite Element Method", 3rd edn. (McGraw-Hill Book Co., New York, 1977).
13. L. J. BROUTMAN and G. PANIZZA, *Int. J. Polym. Mater.* **1** (1971) 95.
14. M. E. J. DEKKERS and D. HEIKENS, *J. Appl. Polym. Sci.* in press.
15. R. H. BECK, S. GRATCH, S. NEWMAN and K. C. RUSCH, *Polym. Lett.* **6** (1968) 707.
16. E. J. HEARN, "Mechanics of Materials" (Pergamon Press, New York, 1977) p. 369.
17. N. J. GOODIER, *J. Appl. Mech.* **55** (1933) 39.
18. A. N. GENT, *J. Mater. Sci.* **15** (1980) 2884.

Received 1 March
and accepted 16 March 1983